COBEM 2023
27TH INTERNATIONAL CONGRESS OF MECHANICAL ENGENEERING

ABCM
Brazilian Society of Mechanical Sciences and Engineering
27th ABCM International Congress of Mechanical Engineering
December 04-08, 2023, Florianópolis-SC, Brazil

COB-2023-0890

SENSITIVITY ANALYSIS OF A NUMERICAL MODEL TO PREDICT POLARIZATION CURVES OF A SOLID OXIDE FUEL CELL AND COMPARISON WITH EXPERIMENTAL RESULTS

Guilherme De Pieri Pickler
Laboratory of Combustion and Thermal Systems Engineering – LabCET, Department of Mechanical Engineering, Federal University of Santa Catarina, Trindade campus, 88040-900 - Florianópolis/SC - Brazil
guilherme.pickler@labcet.ufsc.br

Rafael de Camargo Catapan
Laboratory of Applied Catalysis and Combustion – LAC, Department of Mobility Engineering, Federal University of Santa Catarina – Joinville Campus, 8300 Dona Francisca Street, - North industrial zone - 89219-600 – Joinville/SC - Brazil
rafael.catapan@ufsc.br

Amir Antônio Martins de Oliveira Jr.
Laboratory of Combustion and Thermal Systems Engineering – LabCET, Department of Mechanical Engineering, Federal University of Santa Catarina, Trindade campus, 88040-900 - Florianópolis/SC - Brazil
amir.oliveira@gmail.com

Abstract. *Among the sectors with the highest consumption of non-renewable energy, the transport sector stands out, which currently represents 26.2% of the world's energy balance, with 90% of this consumption being petroleum derivatives. Current engines are considered inefficient compared to other means of energy conversion, such as fuel cells. Predicting the behavior of a fuel cell under embedded operation is crucial to efficiently employ such devices in an efficient way. Therefore, the general objective of this work is to perform a sensitivity analysis of a numeral model to predict polarization curves of a solid oxide fuel cell and compare results against experimental measurements. The mathematical model utilized to predict the polarization curves is collected from literature and written in the software EES. This is a 1-D model based on the flux balance concept and uses the Tafel approximation for fuel cell kinetics. For the experiments, a SOFC fuel cell test system, model 855 from Scribner and a Mellen furnace, Single Stack model were used. The flow rates were measured with a bubblemeter, the inlet pressures were preset at 4 bar and the cell output is linked to the environment. The commercial cell used is a NextCell 7s supported on electrolyte with an active area of 28 cm². The tests were conducted at 1,099, 1,052 and 1,008 K, under flow of* H_2 *and* O_2*. Afterwards, these curves were compared with the 1-D model in EES.* ΔG_{act} *is the parameter it has the greatest influence, when the value was increased by 20% the polarization curve almost disappeared when compared to the other curves. The curves show coherence between the model and the tests for the temperatures of 1,052 and 1,008 K, indicating that 1-D model needs to be improved, possibly including the anode reaction kinetics.*

Keywords: *SOFC, EES, hydrogen, 1-D model, flux balance*

1. INTRODUCTION

Energy is one of the most important inputs in today's world. Despite all efforts, we still have a global energy matrix where the use of non-renewable sources predominates (CNI, 2009). Data from 2020 shows that oil and its derivatives hold the largest share with 29.5%, followed by mineral coal (26.8%) and natural gas (23.7%) (EPE, 2022). Among the sectors with the highest consumption of non-renewable, the transport sector stands out, which currently represents 26.2% of the world's energy balance, with 90% of this consumption being petroleum derivatives (IEA, 2020).

In Brazil there is less dependence on non-renewable sources, which have been replaced in part by energy from hydraulic sources (12.5 %) and biomass (31.4 %), but oil and its derivatives still represent 35.7% of the Brazilian energy matrix. Much of this, driven by the transport sector, which was the sector that consumed the most energy in the country in 2022 with 33% (BEN, 2023). This consumption, even today, is driven mainly by diesel and gasoline, even with the advent of other renewable sources such as biodiesel and ethanol.

Looking at the transport sector, the mass use of internal combustion engines, thermal machines limited in efficiency by the 2nd Law of Thermodynamics, is considered inefficient compared to other means of energy conversion. One of the alternatives to improve performance, both in terms of emissions and energy conversion, is the use of electric vehicles, which can reach 80% efficiency compared to the conventional gasoline vehicles only convert about 12%–30% of the energy stored in gasoline to power at the wheels (FGV Energia, 2017).

However, switching completely from one source of energy to another is still a challenge to be overcome, whether in terms of supply infrastructure, development of new materials or, most importantly, increasing the production of electricity on the grid. One of the ways to use electric vehicles and still use fuels, but without relying on internal combustion engines, is through the so-called fuel cells, which are electrochemical devices, that is, they directly convert the chemical energy of fuels into electrical energy, not being limited by the Carnot efficiency. As a result, they have efficiencies that can exceed 60% of energy use (Kordesch and Simader, 1996). Currently, fuel cells are presented as important alternatives for application in the transport sector, with the potential to solve problems considered critical in electric vehicles, such as: supply, energy storage and autonomy (FGV Energia, 2017).

Of the existing types of fuel cell, two are more suitable for vehicle operation: PEM (Proton Exchange Membrane) and SOFC (Solid Oxide Fuel Cell) cells, the latter having the advantage of being able to work with other types of fuels in addition to hydrogen, such as for example ethanol, a biofuel (Shuai Ma et al., 2021). Predicting the behavior of a fuel cell under embedded operation is crucial to efficiently employ such devices in an efficient way.

Numerous processes occur in a fuel cell, among them momentum, heat, and mass transfer, along with electrochemical reactions. All these processes result in a set of complex equations that need to be analyzed carefully so that suitable numerical methods can be used to solve them (Sreedhar et al, 2019). Mathematical modeling is a crucial tool in the study of fuel cell behavior and performance. It assists in control strategies and design experiments. Simulation results need to be experimentally validated to ensure credibility. Solid oxide fuel cells can be categorized based on cell and stack design, support type, flow configuration, temperature level and type of fuel reform (Colpan et al, 2008). 1-D planar models and tubular models have been extensively studied along with 2-D and 3-D to analyze various momentum, heat and mass transfers, apart from electrochemical processes, and other balances and reactions. Below are some examples of studies carried out.

Lu et al. (2006), developed a 0-D model with transient nature to discuss the thermal and electrochemical dynamics inside SOFC APU (Auxiliary Power Unit) and responses to load changes. Gebregergis et al. (2009), studied a tubular 0-D lumped model and compared it to distributed model with equal partial pressures.

Haynes (2004) simulated unrestrained load response characteristics using 1-D or 0-D tubular transient SOFC. Xue et al. (2005), studied a 1-D model of steady state nature. Their model was of tubular design. They observed that non-uniform partial pressures and temperature distribution cause non-uniform contribution and Nernst potential distribution. A planar 2-D SOFC was modeled by Beale et al. (2003).

In modeling studies, computational times and accuracy in predictions were very important factors and as the complexity of the models increases, there is a need for more computational power. Currently, in these cases, authors usually employ a 3-D model. Yakabe et al. (2000), modeled a planar 3-D SOFC and found that when fuel utilization is high, shift reaction reduces concentration polarization considerably. A 3-D planar model designed by Recknagle et al. (2003), suggests that for a given temperature distribution, similar fuel utilization can take place for any flow. Bae et al. (2018) have developed a three-dimensional dynamic model to study the impact of electrical load change on thermodynamic variables related to SOFC thereby on achieving reliable cell microstructure and stack design to enhance their stability and durability which are critical for their large-scale deployment.

To reduce computational times and costs, two approaches are generally followed viz., reducing 3D models to lower dimensional models (2-D or 1-D) and even 0-D or blackbox models using lumped parameters and by writing electrochemical reactions at the three-phase interface of the electrolyte. While the former approach is faster but of low accuracy, the latter approach requires good simulation software. There are also multidimensional models, a combination of reduced dimensions and reduced physics being developed in the recent past which gave novel, effective and faster solutions. Ghorbani and Vijayaraghavan (2018) have developed a simplified pseudo-2D model for a planar SOFC module which had low computational times and compared the results with those of a 3D model. They found that there was a good agreement between the results and hence this simplified model that was even validated with experimental data could be used for both online diagnosis and to design effective control strategies. Kishimoto et al. (2021) divided the practical-size cell into independent one-dimensional (1-D) unit cells and evaluated the characteristics of the practical-size cell as an aggregation of the performance of local unit cells. For this purpose, a 1-D numerical simulation model is developed and validated by comparing the predicted values with experimental data. It is confirmed that not only the current–voltage characteristics but also the impedance characteristics are accurately reproduced by the developed unit cell model.

Based on what has been exposed so far, the general objective of this work is to perform a sensitivity analysis of a numeral model to predict polarization curves of a solid oxide fuel cell and compare results against experimental measurements.

This work started with a 1-D model present in literature and detailed by O'Hayre et al. (2016) in his book. The model, based on flux balance, was implemented in the EES (Engineering Equation Solver) using the initial data from experiments to obtain the polarization curves. Afterwards, these curves were compared with experimental data obtained from testing a commercial solid oxide fuel button cell fed with H_2 and O_2. From this, exhaustive analyzes were carried out to measure the sensitivity of the model and its parameters.

2. NUMERICAL MODEL

To determine the operating voltage and power of a fuel cell it will be necessary to determine the influence of the losses on the thermodynamic voltage:

$$V = E_{thermo} - \eta_{act} - \eta_{ohm} - \eta_{conc}, \tag{1}$$

$$P = V.j, \tag{2}$$

where V is the operating voltage of fuel cell, E_{thermo} is the thermodynamically predicted voltage of fuel cell, η_{act} is the activation losses due to reaction kinetics, η_{ohm} is the ohmic losses from ionic and electronic resistance, η_{conc} is the concentration loss due to mass transport, j is the current density and P is the power supplied by the fuel cell. The combined effect of the influences, relative to the various cargo losses, will determine the behavior of the fuel cell, that is, the performance of the fuel cells will be related to these losses.

This model is based on the flux balance concept and uses the Tafel approximation for fuel cell kinetics, that is, when the activation losses are large (50-100 mV) or, more fundamentally, when $j \gg j_0$. (O'Hayre et al., 2016). Flux balance allows us to keep track of all the species that flow in, out, and through a fuel cell. To generate an accurate 1-D flux balance fuel cell model, the fluxes of all chemical species going into, out of, and through the fuel cell must be detailed. Figure 1 illustrates the high-level flux detail needed in our 1-D fuel cell model. This diagram essentially allows us to keep track of the H_2O and H_2 flowing into/out of the anode, the N_2, and O_2 flowing into/out of the cathode, and the O^{2-} flowing across the electrolyte membrane.

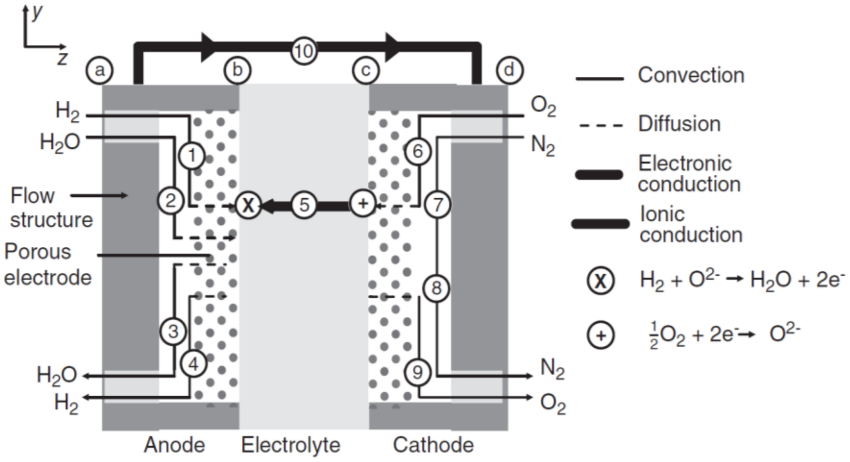

Figure 1. Flux details for 1D SOFC model. In a SOFC, oxygen ions (O^{2-}) transport through the electrolyte (O'Hayre, 2016).

The fluxes in Figure 1 can be related to one another using the principle of *flux balance* — the *current density*, or charge flux of the fuel cell. And for a SOFC the flux balance equation as shown as below

$$\frac{j}{2F} = J^{M}_{O^{2-}} = J^{A}_{H_2} = 2J^{C}_{O_2} = -J^{A}_{H_2O}, \tag{3}$$

where F is the Faraday's constant, and J is the molar flux. M, A and C represent the membrane, anode, and cathode, respectively.

To reduce the modeling requirements some simplifying assumptions are listed below:

- Advective transport is ignored. This model is a 1-D model, so convection can be safely ignored. As Figures 1 indicates, convective transport is mostly along the y-axis, but in this 1D model it is considered transport only along the z-axis.
- Diffusive transport in the flow channels is ignored. In the flow channels, diffusion is far less dominant than convection.
- All the ohmic losses come from the electrolyte membrane. For most fuel cells, this is a reasonable assumption, because the ohmic losses from ionic conduction in the electrolyte tend to dominate the other ohmic losses.
- The anode reaction kinetics are ignored. In H_2–O_2 fuel cells, the anode activation losses are usually much smaller than the cathode activation losses since oxygen reduction is the most sluggish process.

- The catalyst layers are extremely thin or act as "interfaces" (no thickness). In most SOFCs, however, the catalyst layer and electrode form a single unified body. Ionic conduction and electrochemical reactions may happen throughout the entire thickness of the electrode. Usually, however, reactions are localized to a very thin region of the catalyst/electrode bordering the electrolyte. In this case, the assumption is still justified.
- The water exists only as water vapor. For SOFCs, this assumption is justified; only water vapor will exist at typical SOFC operating temperatures.

The assumptions described above in the text should be used only for cathode- and electrolyte-supported SOFCs, as described by O'Hayre et al. (2016).

2.1 Governing Equations

By solving the governing equations, it's possible to determine how the concentrations of H_2, O_2, H_2O, and N_2 vary across the fuel cell (in the z direction) and with this calculate the mass transport overvoltage η_{conc}, activation overvoltage η_{act}, and ohmic overvoltage η_{ahm} at different current density levels j. Then, with all these parameters, to construct a j–V curve.

Electrode:

To model the diffusion processes for H_2, O_2, H_2O, and N_2 a modified form of the basic diffusion model (Springer et al., 1991) was used,

$$J_i = \frac{-pD_{ij}^{eff}}{RT}\frac{dx_i}{dz}, \tag{4}$$

where x_i stands for the mole fraction of species i, p is the total gas pressure at the electrode, R is the ideal gas constant, T is the temperature of the gas and D_{ij}^{eff} is the effective diffusivity. This equation can be integrated using the ideal gas law. At high temperatures a correlation is used to give effective diffusivity (Cussler, 1995).

$$D_{ij}^{eff} = D_{ij}\frac{\varepsilon}{\tau}, \tag{5}$$

where ε is *porosity* of the porous structure, fuel cell electrodes have porosities of around 0.4 (porosity represents the ratio of pore volume to total volume). τ is the tortuosity, it is known that tortuosity can vary from 1.5 to 10, depending on pore structure configuration (tortuosity describes the additional impedance to diffusion caused by a tortuous or convoluted flow path). D_{ij} is the binary diffusion coefficient that can be estimated from the following equation based on the kinetic theory of gases (at low pressures) (Bird et al., 2002).

$$p \cdot D_{ij} = a\left(\frac{T}{\sqrt{T_{ci}T_{cj}}}\right)^{b}\left(p_{ci}p_{cj}\right)^{\frac{1}{3}}\left(T_{ci}T_{cj}\right)^{\frac{5}{12}}\left(\frac{1}{M_i}+\frac{1}{M_j}\right)^{\frac{1}{2}}, \tag{6}$$

where M_i, M_j are the molecular weights of species i and j, and T_{ci}, T_{cj}, p_{ci}, p_{cj} are the critical temperatures and pressures of species i and j. Typically, use a = 2.745x10^{-4} and b = 1.823 for pairs of nonpolar gases, such as H_2, O_2, and N_2. For pairs involving H_2O (polar) and a nonpolar gas, one can use a = 3.640x10^{-4} and b = 2.334 (Bird et al., 2002).

Electrolyte:

For SOFCs, the important is the O^{2-} flux across the electrolyte. From the flux balance (Equation 3) it is possible to relate the O^{2-} flux to the current density:

$$J_{O^{2-}}^{M} = \frac{j}{2F}, \tag{7}$$

Then, the ohmic voltage loss can be determined (O'Hayre et al., 2016):

$$\eta_{ohm} = j(ASR_{ohmic}) = j\left(\frac{t^M}{\sigma}\right), \tag{8}$$

where t^M is the thickness of the electrolyte. To calculate the electrolyte conductivity σ, the following equation is used:

$$\sigma = \frac{A_{SOFC}e^{\frac{-\Delta G_{act}}{(RT)}}}{T}, \tag{9}$$

where A_{SOFC} is a is a preexponential factor and ΔG_{act} is the activation energy for ion migration and both are usually obtained from experiment.

Catalyst:

Here, only the cathode reaction kinetics is considered. Since the oxygen partial pressure at the cathode is the dominant factor in determining the cathodic overvoltage and using the simplified form of the Butler–Volmer equation for an ideal gas (O'Hayre et al., 2016) the equation becomes:

$$\eta_{cathode} = \frac{RT}{4\alpha F} ln \, \frac{j}{j_0 p^c x_{O_2}}, \tag{10}$$

where α is the charge transfer coefficient, j_0 is the exchange current density, p^c is the total pressure at the cathode and x_{O_2} is the oxygen mole fraction at the cathode catalyst layer. Here, the 4 in the denominator represents the electron transfer number for an oxygen molecule. As the oxygen concentration was considered in this equation, it is effectively accounting for both activation losses and concentration losses at the same time.

From equation (4) and (7) it is possible to relate $J^M_{O^{2-}}$ to the fuel cell current density j. Then one can obtain the oxygen profile at the cathode and hence the oxygen concentration at the cathode catalyst layer (cross section c in Figure 1):

$$x_{O_2}|_c = x_{O_2}|_d - t_c \frac{jRT}{4Fp^c D^{eff}_{O_2,N_2}}, \tag{11}$$

where t_c is the thickness of the cathode, $x_{O_2}|_d$ is the oxygen concentration in the cross section d (Figure 1), a boundary condition.

Now consider a more realistic case where oxygen can be depleted at boundaries depending on the relative rates of oxygen supply and consumption.

$$x_{O_2}|_d = \frac{\lambda_{O_2}-1}{(1+\omega)\lambda_{O_2}-1}, \tag{12}$$

where ω represents the molar ratio of nitrogen to oxygen in air and λ_{O_2} is the stoichiometric number, that reflects the rate at which a reactant is provided to a fuel cell relative to the rate at which it is consumed. For example, $\lambda = 2$ means that twice as much reactant as needed is being provided to a fuel cell.

Reversible cell voltage:

The reversible cell voltage is the maximum value of voltage that can be achieved. The full expression describing how the reversible cell voltage varies with temperature, pressure, and activity (concentration), was mentioned at O'Hayre et al. (2016). But the activity can be replaced by the partial pressures of the gases in the reaction. As here it was considered a hydrogen–oxygen fuel cell reaction the equation can be written as

$$E_{thermo} = E^0 + \frac{\Delta \hat{s}}{nF}(T - T_0) - \frac{RT}{nF} ln \, \frac{p_{H_2O}}{p_{H_2} p_{O_2}^{1/2}}, \tag{13}$$

where E^0 is the reversible voltage under standard-state conditions, n is number of moles of electrons transferred (for a reaction H_2-O_2, n = 2), $\Delta \hat{s}$ is the change in entropy of the reaction, T_0 is the reference temperature, p_{H_2O} is the partial pressure of water (vapor state), p_{H_2} is the partial pressure of hydrogen and p_{O_2} is the partial pressure of oxygen. Even if air is used nitrogen (N_2) is inert and should not be included.

2.2 Initial data

To solve the 1-D model a script was written in the software EES (Engineering Equation Solver). The initial data, process and material parameters required are shown in Table 1.

Table 1. Initial data and physical properties of SOFC used in 1-D model.

Properties	Values	References
Temperature [T], K	1099	-
Oxygen inlet mole fraction [$x_{O_2}|_d$], -	0.99	(White Martins)
Cathode pressure [p^c], atm	4	(Scribner Associates Inc.)
Electrolyte thickness [t^M], µm	150	(Arias, 2012)
Cathode thickness [t_c], µm	50	(Arias, 2012)
Gas constant [R], J/mol.K	8.314	-
Faraday constant [F], C/mol	96,485	-
Reference temperature [T_0], K	298	-
Reference pressure [p_0], atm	1	-

Molar mass of oxygen [M_{O_2}], g/mol	31.999	-
Molar mass of nitrogen [M_{N_2}], g/mol	28.013	-
Critical temperature of oxygen [$T_{c_{O_2}}$], K	154.4	-
Critical temperature of nitrogen [$T_{c_{N_2}}$], K	162.2	-
Critical pressure of oxygen [$p_{c_{O_2}}$], atm	49.7	-
Critical pressure of nitrogen [$p_{c_{N_2}}$], atm	33.5	-
Diffusibility constant a, -	2.745x10^{-4}	(O'Hayre et al., 2016)
Diffusibility constant b, -	1.823	(O'Hayre et al., 2016)
Porosity [ε], -	0.4	(O'Hayre et al., 2016)
Tortuosity [τ], -	1.5	(O'Hayre et al., 2016)
Reversible voltage under standard-state conditions [E^0], V	1,23	Kordesch, K. Simader, G., 1996.
Stoichiometric number [λ], -	2	(O'Hayre et al., 2016)
Entropies [$\hat{s}_{O_2}$, $\hat{s}_{H_2}$, $\hat{s}_{H_2O}$], J/mol.K	EES thermodynamic tables	-
The active area of the cell [A_{cell}], cm²	28	(Arias, 2012)

There are 4 parameters whose behavior is unknown under the established conditions, so they were chosen to be varied in the tests of the program to carry out the sensitivity analysis: A_{SOFC}, ΔG_{act}, j_0 and α. They have a standard value from O'Hayre (2016), as shown in Table 2, but is common for these parameters to change their values depending on the kind of SOFC, the materials and substances used in the cathode, anode and electrolyte.

Table 2. Standard values for the parameters chosen for the sensitivity analysis.

Properties	**Standard Values**
Preexponential factor [A_{SOFC}], K/Ω.m	9.0×10^7
Activation energy [ΔG_{act}], kJ/mol	100
Exchange current density [j_0], A/m²	1000
Charge transfer coefficient [α], -	0.5

3. EXPERIMENTAL

The compare the results of the 1-D model described above, some tests were conducted on an experimental bench. A commercial NextCell 7s Electrolyte Supported Cells (NexTech Materials Inc., USA) was purchased, which use conventional materials for SOFC processing, as shown in Table 3. The active area of the cell is 28 cm² (5×6 cm).

Table 3. NetxCell 7s SOFC specifications (Arias, 2012).

	Anode	**Electrolyte**	**Cathode**
Material	Ni-YSZ⁽¹⁾	YSZ	LSM⁽²⁾
Thickness, µm	50	150	50
Area, cm²	28	100	28

(1) Nickel and Yttria-stabilized zirconia
(2) Lanthanum strontium manganite

The electrochemical characterization of the cell was performed on an 855 SOFC Test System from Scribner Associates Inc., USA. The cells are placed in a furnace (Mellen Inc., USA) using a fixture in stainless steel, where the flows are drawn for the anode and the cathode. The tests are run at 4 atm of pressure (minimum required by the system 855) and the gases are freely discharged to the atmosphere. To control the flows of oxidant (O_2 > 99,5% - White Martins, Brazil), fuel (H_2 > 99,95% - White Martins, Brazil) and the inert gas for dilution in the anode (N_2 > 99,998% - White Martins, Brazil) some needle valves from Swagelok are used and to pre-set the volumetric flow a bubble meter was used in the line of gases. An image of the bench for testing SOFC is shown in Figure 2.

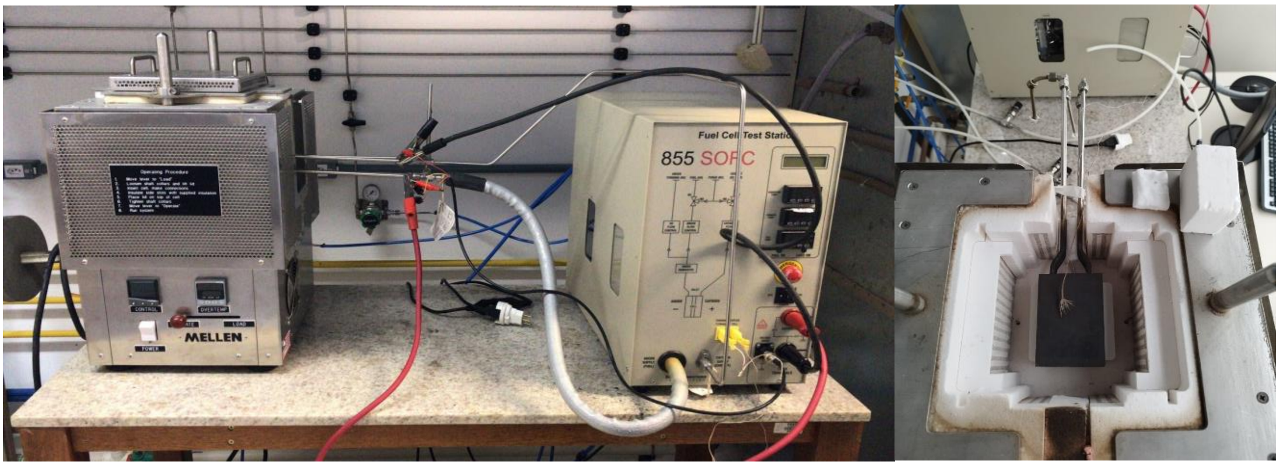

(a) (b)

Figure 2. Experimental setup for the electrochemical tests (a) and the cell assembled inside the furnace (b).

Before starting the tests, a cell conditioning is recommended by the manufacturer: to program furnace to heat up to 1,123 K in 14 hours (~1°C/min) and hold at 1,123 K, during this keep a flowrate of air/O_2 in the cathode (350 ml/min) and N_2 in the anode (350 ml/min).

Following the instructions of the FuelCell Materials (division of NexTech Materials) the nickel in the anode of the cells as received was in the form of oxide, so it was reduced using a mixture of 15% hydrogen in nitrogen after the cell conditioning. This procedure is performed to stabilize the cell before testing and to increase the porosity of the anode (Arias, 2012). The temperature for the reduction was 1,123 K, the flow in the cathode was O_2 at 350 ml/min, and in the anode the total flow was 260 ml/min. Nitrogen was initially used, and gradually replaced by the hydrogen mixture, according to the change in the open circuit voltage. That is, only slight OCV (open circuit voltage) changes were allowed during reduction, by controlling the addition of hydrogen. After reduced, the cell was electrochemically tested just using H_2 (anode) and O_2 (cathode) at 3 different temperatures: 1,099, 1,052 and 1,008 K. The initial intention was to start with 850 ºC and decrease by 50 ºC. But temperature stabilization was not easy to achieve.

4. RESULTS AND DISCUSSION

In this section it will show the results for the experiments and the 1-D model, then a comparison between both is made. The analysis of the results passes through the sensitivity analysis of some parameters that are important for fuel cells.

4.1 Experimental results

After cell conditioning and cell reduction the flow was set to 260 ml/min for H_2 and 1370 ml/min to O_2, near to the flow solicited in the instructions of the FuelCell Materials. More accurately flows are limited to the error in the bubble meter. When the OCV (open circuit voltage) was stabilized, the tests began. Figure 3 shows the results for the 3 temperatures proposed.

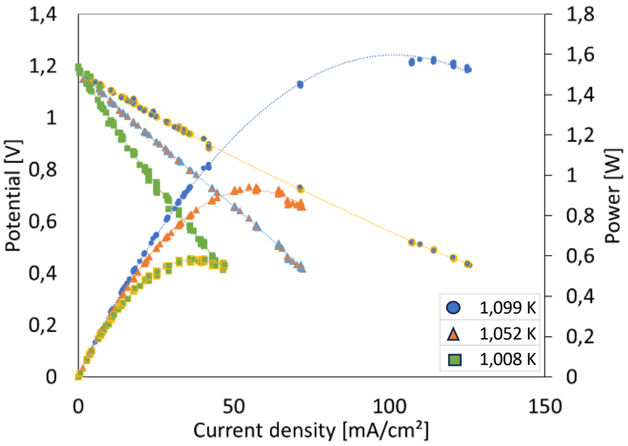

Figure 3. Polarization and power curve.

It is possible to verify from the results that with the increase in temperature there is also an increase in the power and voltage generated, which is in line with what is reported in the literature. The shape of the curves is also consistent with what is observed in the literature, but the maximum values obtained are not, indicating a possible limitation of the commercial cell.

4.2 1-D model results and sensitivity analysis

As O'Hayre (2016) comments, A_{SOFC} and ΔG_{act} are obtained from experiments. The value of α is always between 0 and 1. For "symmetric" reactions, α = 0.5. For most electrochemical reactions, α ranges from about 0.2 to 0.5. The exchange current density j_0 measures the equilibrium rate at which reactant and product species are exchanged in the absence of an activation overvoltage. A high j_0 indicates a facile reaction, while a low j_0 indicates a sluggish reaction.

To understand how each parameter influences the polarization and power curve it was proposed a variation of +/- 20% in the standard values following a similar approach from Wehrle et al. (2022). While one parameter varies, the others remain at the default value. Figure 4 shows the standard curves and their variations.

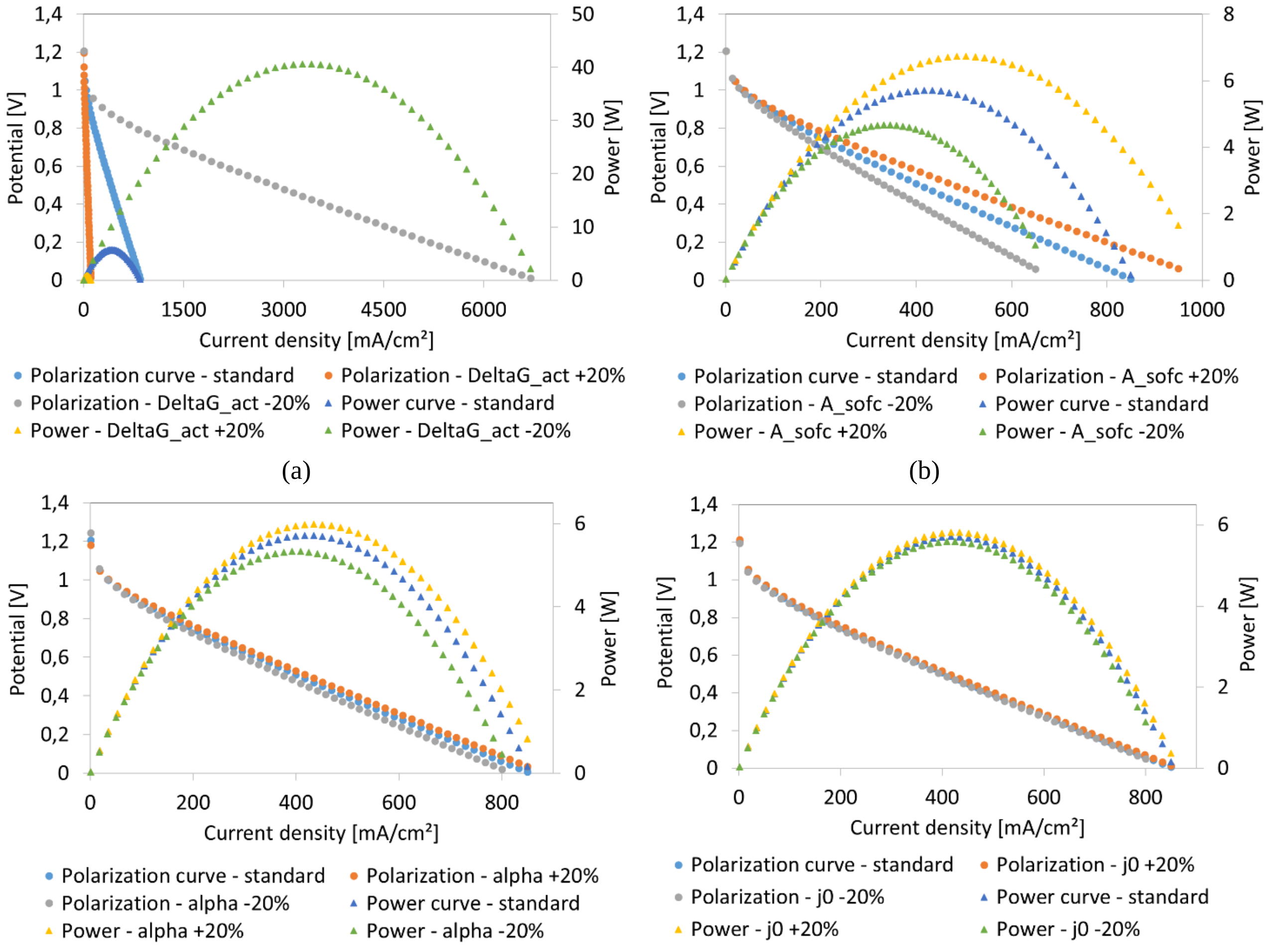

(a) (b)

(c) (d)

Figure 4. Comparison between polarization and power curves for (a) ΔG_{act}, (b) A_{SOFC}, (c) α and (d) j_0.

Through the presented results it is possible to observe that ΔG_{act} has the greatest influence when changed. ΔG_{act} is the activation barrier for the diffusion process and the size of it is often critical for determining the conductivity of SOFC electrolytes. To change the activation barrier, it is necessary to change the free-energy surface of the reaction, which depends on the nature of the electrode metal and the fluids involved in the reaction. Typically, its value ranges between about 50,000 and 120,000 J/mol (O'Hayre et al., 2016). When the value was increased by 20% the curve almost disappeared when compared to the others, representing that, this parameter is inversely proportional to the voltage and power, that is, the higher the barrier, the lower the conduction of electrolytes.

A_{SOFC} is the second greatest influence, but it is directly proportional to the voltage and power. The results show that increasing A_{SOFC} there is a better cell performance, this can be achieved creating high vacancy concentrations by intentional doping. A_{SOFC} is pseudo-empirical value that groups the various preexponential terms into a single factor, like concentration of lattice sites for the species of interest in the material and diffusivity. This parameter is related to material's conductivity which is determined by the product of carrier concentration and carrier mobility. These properties are, in turn, set by the structure and conduction mechanisms within the material.

The changes made to j_0 and α did not represent large changes in the curves and they are directly proportional. Both are parameters that are part of the activation e concentration losses and, their influence is more significant in the beginning and final part of the polarization curve.

Activation overvoltage losses are minimized by maximizing j_0. There are four major ways to increase j_0: (1) increase reactant concentration, (2) increase reaction temperature, (3) decrease the activation barrier (by employing a catalyst), and (4) increase the number of reaction sites (by fabricating high-surface-area electrodes and 3D structured reaction interfaces).

The Butler–Volmer equation predicts that increasing α will result in a higher net current density. Therefore, catalysts with a high α should be desired over catalysts with a low α, such as Pt, Pd, Ir, and Rh. Generally, α is difficult to quantify and changes only slightly with choice of catalyst, so it is often overlooked compared to other catalytic effects.

4.3 Comparison between 1-D model and experimental tests

It is now known how these parameters influence the 1-D model and it is possible to change them to find a better combination that agrees with the experimental tests.

From the sensitive analysis of the previous section, it was verified that ΔG_{act} is the parameter that most influences the 1-D model. From this, a series of trials and errors began to better adapt the curve just by varying this parameter. Then, the same process was repeated for A_{SOFC}, α and j_0, respectively, starting from the most influential parameter to the least influential one. During this process, some adjustments were made in the previous parameters to correct curve deviations.

Therefore, after several attempts were made to reach a better combination of these parameters, the results can be seen in Table 4, Figure 5.

Table 4. Values found for the analyzed parameters.

Properties	**Values**
Preexponential factor [A_{SOFC}], K/Ω.m	8.9×10^{7}
Activation energy [ΔG_{act}], kJ/mol	114
Exchange current density [j_0], A/m²	850
Charge transfer coefficient [α], -	0.65

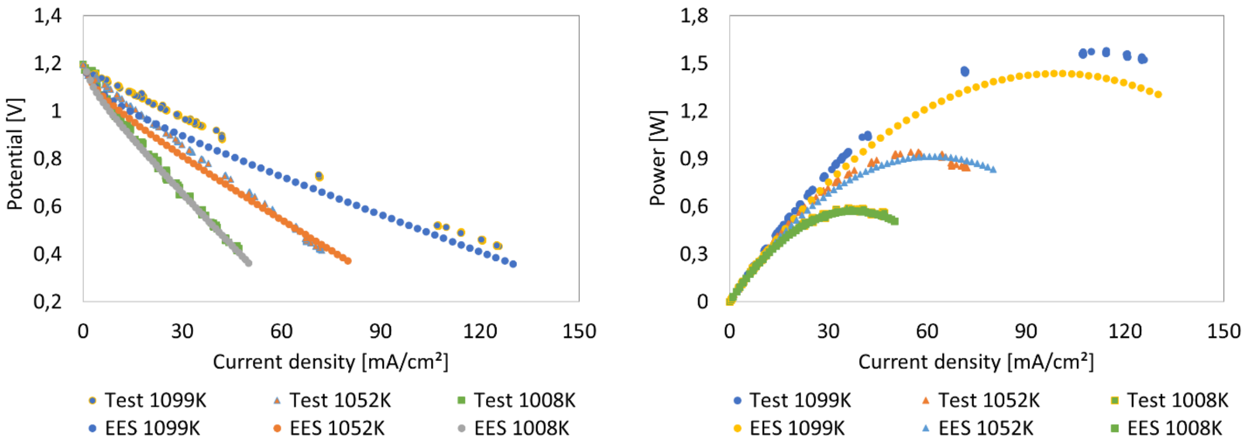

Figure 5. Polarization and power curve - Comparison between tests and 1-D model.

For lower temperatures the model presents good agreement with the experimental results, but for higher temperatures it has a certain discrepancy in the curves. As this is a 1-D model, a lot of assumptions and simplifications were made, so it has limitations to hit all the points. Convective transport and diffusive transport in the flow channels is ignored, increasing the temperature these plots tend to be more significant.

Another point that can be mentioned is that in the experimental tests the voltage drops very fast initially with the increase of j, and the model cannot predict this. That is, the activation losses end up being underestimated, probably because the anode reaction kinetics are ignored, and we assume that the catalyst layers are extremely thin or act as "interfaces" (no thickness) and this is not true.

5. CONCLUSIONS

The sensitivity analysis of a numeral model to predict polarization curves of a solid oxide fuel cell was made and the results were compared against experimental measurements. 4 parameters were analyzed, ΔG_{act}, A_{SOFC}, α and j_0. The first two are linked to ohmic losses and have the greatest influence on the polarization curves. The others are linked to activation and concentration losses, with a more pronounced influence at the beginning of the curves.

This is a preliminary study to understand the functioning of the experimental apparatus and the behavior of a SOFC foreseeing soon the implementation of MS-SOFC and integrated reformer in the same mathematical model. A good agreement between the model and tests was observed to the temperatures of 1,052 and 1,008 K. But the 1-D model needs improvement to work well at other temperatures.

As future works it is suggested the implementation in the mathematical model of the kinetic reactions of the anode. In the experimental part, different temperatures, and flow rates of H_2 and O_2 can be analyzed.

6. REFERENCES

Aguiar, P. Chadwick, D. Kershenbaum, L. Modelling of an indirect internal reforming solid oxide fuel cell. Chemical Engineering Science, 2002, 57 (10), 1665–1677.

Arias, J. L. A. Células a combustível de óxido sólido planares: Processamento e avaliação do desempenho usando álcool como combustível. Tese. Federal University of Santa Catarina, 2012.

Bae, Y. Lee, S. Yoon, K. J. Lee, J. H. Hong, J. Three-dimensional dynamic modeling and transport analysis of solid oxide fuel cells under electrical load change Energy Conversion and Management, 2018, 165, 405–418.

Beale, S. B. Lin, Y. Zhubrin, S. V. Dong, W. Computer methods for performance prediction in fuel cells. Journal of Power Sources, 2003, 118 (1–2), 79–85.

Bird, R. Stewart, W. Lightfoot, E. Transport Phenomena, 2nd ed. John Wiley & Sons, New York, 2002.

CNI, 2009. *Energy efficiency in industry* (in Portuguese). Confederação Nacional da Indústria, Brasília, 16 p.

Colpan, C. O. Dincer, I. Hamdullahpur, F. A review on macro-level modeling of planar solid oxide fuel cells. International Journal of Energy Research, 2008, 32 (4), 336–355.

Cussler, E. L. Diffusion: Mass Transfer in Fluid Systems. Cambridge University Press, Cambridge, 1995.

EPE, 2023, *National Energy Balance 2023, Final Report* (in Portuguese), Empresa de Pesquisa Energética EPE, Rio de Janeiro, https://www.epe.gov.br/sites-pt/publicacoes-dados-abertos/publicacoes/PublicacoesArquivos/publicacao-748/topico-687/BEN2023.pdf. Accessed 31 August 2023.

EPE, 2022. *Energy and electrical matrix* (in Portuguese), Empresa de Pesquisa Energética EPE, Rio de Janeiro, www.epe.gov.br/pt/abcdenergia/matriz-energetica-e-eletrica#TOPO. Accessed 15 December 2022.

INTERNATIONAL ENERGY AGENCY. IEA Sankey Diagram. Paris, 2022, https://www.iea.org/sankey/. Accessed 12 December 2022.

FGV, 2017. *Electric Cars* (in Portuguese). FGV ENERGIA, Rio de Janeiro, https://fgvenergia.fgv.br/sites/fgvenergia.fgv.br/files/caderno_carros_eletricos-fgv-book.pdf. Acessed 12 December 2022.

FuelCell Materials. Instructions for Loading Single Cell with 28 cm² active area. Nexceris, Ohio, USA, https://fuelcellmaterials.com/wp-content/uploads/28-cm2-cell-kit-instructions.pdf. Accessed 14 October 2022.

Gebregergis, A. Pillay, P. Bhattacharyya, D. Rengaswemy, R. Solid Oxide Fuel Cell Modeling. IEEE Transactions on Industrial Electronics, 2009, 56 (1), 139–148.

Ghorbani, B. Vijayaraghavan, K. 3D and simplified pseudo-2D modeling of single cell of a high temperature solid oxide fuel cell to be used for online control strategies. International Journal of Hydrogen Energy, 2018, 43 (20), 9733–9748.

Haynes, C. Simulating process settings for unslaved SOFC response to increases in load demand. Journal of Power Sources, 2002, 109 (2), 365–376.

Kishimoto, M. Kishida, S. Seo, H. Iwai, H. Yoshida, H. Prediction of electrochemical characteristics of practical-size solid oxide fuel cells based on database of unit cell performance. Applied Energy 2021, 283: 116305.

Kordesch, K. Simader, G., 1996. Fuel Cells and Their Applications, VCH, Weinheim. ISBN 3-527-28579-2

Lu, N. Li, Q. Sun, X. Khaleel M. A. The modeling of a standalone solid-oxide fuel cell auxiliary power unit. Journal of Power Sources, 2006, 161 (2), 938–948.

Ma, S. Lin, M. Lin, T. Lan, T. Liao, X. Maréchal, F. Van Herle, J. Yang, Y. Dong, C. Wang, L, 2021. Fuel cell-battery hybrid systems for mobility and off-grid applications: A review. Renewable and Sustainable Energy Reviews. Elsevier. Volume 135, 110119.

O'Hayre, R. P., Cha, Suk-W., Colella, W., Prinz, F. B. Fuel Cell Fundamentals. Third Edition, 2016. John Wiley & Sons, Inc.

Recknagle, K. P. Williford, R. E. Chick, L. A. Rector, D. R. Khaleel, M. A. Three-dimensional thermo-fluid electrochemical modeling of planar SOFC stacks. Journal of Power Sources, 2003, 113 (1), 109–114.

Springer, T. E. Zawodzinski, T. A. Gottesfeld, S. Polymer electrolyte fuel cell model. Journal of the Electrochemical Society, 138(8): 2334–2342, 1991.

Sreedhar, I. Agarwal, B. Goyal, P. Singh, S. A. Recent advances in material and performance aspects of solid oxide fuel cells. Journal of Electroanalytical Chemistry, 2019, 848, 113315

Wehrle, L. Wang, Y. Boldrin, P. Brandon, N. P. Deutschmann, O. Banerjee, A. Optimizing solid oxide fuel cell performance to re-evaluate its role in the mobility sector. ACS Environmental Au. 2022 2 (1), 42-64 DOI: 10.1021/acsenvironau.1c00014

Xue, X. Tang, J. Sammes, N. Du, Y. Dynamic modeling of single tubular SOFC combining heat/mass transfer and electrochemical reaction effects. Journal of Power Sources, 2005, 142 (1–2), 211–222.

Yakabe, H. Hishinuma, M. Uratani, M. Matsuzaki, Y. Yasuda, I. Evaluation and modeling of performance of anode-supported solid oxide fuel cell. Journal of Power Sources, 2000, 86 (1–2), 423–431.